

Lehigh University Lehigh Preserve

Fritz Laboratory Reports

Civil and Environmental Engineering

1975

K-value analysis for cracks in bridge structures, June 1975

H. Tada

G. R. Irwin

Follow this and additional works at: <http://preserve.lehigh.edu/engr-civil-environmental-fritz-lab-reports>

Recommended Citation

Tada, H. and Irwin, G. R., "K-value analysis for cracks in bridge structures, June 1975" (1975). *Fritz Laboratory Reports*. Paper 2116. <http://preserve.lehigh.edu/engr-civil-environmental-fritz-lab-reports/2116>

This Technical Report is brought to you for free and open access by the Civil and Environmental Engineering at Lehigh Preserve. It has been accepted for inclusion in Fritz Laboratory Reports by an authorized administrator of Lehigh Preserve. For more information, please contact preserve@lehigh.edu.

399.1

K-VALUE ANALYSIS FOR CRACKS IN BRIDGE STRUCTURES

(ROUGH DRAFT REVIEW COPY)

by

H. Tada

G. R. Irwin

**FRITZ ENGINEERING
LABORATORY LIBRARY**

June 1975

Fritz Engineering Laboratory Report No. 399.1

TABLE OF CONTENTS

	Page
INTRODUCTION	1
1. TWO-DIMENSIONAL EDGE CRACK PROBLEMS	4
A. An Edge Crack in Half-Plane (Straight Free Boundary)	4
B. An Edge Crack in Half-Plane (Free Boundary Consists of Two Straight Lines)	9
C. An Edge Crack in a Long Strip	11
2. THE HALF-CIRCLE AND QUARTER-CIRCLE SURFACE CRACKS	16
A. A Circular Crack in an Infinite Body	16
B. The Half-Circle Surface Crack and the Quarter- Circle Corner Crack	20
3. ELLIPTICAL SURFACE CRACKS	33
A. Method A	35
B. Method B	37
C. Free Surface Correction Factors	41
4. SUMMARY	44
5. REFERENCES	45
A. References Directly Used in the Report	
B. Other References	

INTRODUCTION

As a portion of the DOT project at Lehigh University entitled "Tolerable Flaw Sizes in Full Scale Bridge Weldments", crack shapes and structural complexities of various cracks which may be encountered in this project have been studied from the viewpoint of analytical treatment. Exact analytical treatment of natural cracks in service components has never been possible. The first goal of the analytical work is to predict K-values for the cracks studied in this project with enough accuracy to permit an understanding of the fracture failures in terms of failure load and fracture toughness. A second goal of the analytical study is to develop simplified methods of dealing with the influences of structural complexities commonly associated with bridge structure cracks. It is believed that the methods discussed in this report will prove satisfactory with regard to the first objective. Since the two goals are related, some comments on simplification of K-estimate methods will be included.

Two-dimensional problems involving one or two free edges and various stress distributions are discussed first. These results are of value for direct use in the case of through-the-thickness cracks. In addition they provide perspective with regard to the interaction between free surface effects and stress distribution. Three-dimensional crack problems are much more complex. The half-elliptical crack extending directly into a plate from a single free surface was

first discussed in 1962 (1). Increased interest in this problem led to enough analytical and experimental results so that approximate K-estimates for uniform tension and uniform bending can be made with some confidence.

A useful proposal for making estimates of this kind in terms of semi-empirical equations has been furnished by Merkle (2,3). In the case of surface cracks which have a large surface length-to-depth ratio (greater than 6), K-values for the central region of major interest can usually be understood in terms of a two-dimensional analysis. For the cracks with smaller surface length-to-depth ratio, the accuracy of Merkle's equation should be on the order of $\pm 5\%$, an adequate degree of precision for this project. In the case of residual stress fields which cannot be closely approximated as a combination of uniform bending and uniform tension, use of Merkle's equation becomes very complex. Study has therefore been given to a weight factor approach to K-value estimates for three-dimensional surface cracks of elliptical contour. This approach is based upon the exactly known K-value weight factors for the case of pairs of splitting forces acting on the surfaces of a circular disc crack in an infinite plate. Using these as a guide, approximate weight factor functions were estimated and explored for pairs of splitting forces acting on the surfaces of a flat elliptical crack in an infinite plate. A satisfactory degree of accuracy was obtainable with a relatively simple weight function when the ratio of the semi-axes of the crack was less than 3 (corresponding to surface length-to-depth ratio less than 6 for a surface crack). Calculations of K-values at several points of interest

on the crack boundary were made for a variety of stress distributions. Comparison of these results to results obtained using the Merkle equation and to K-value results otherwise available suggest approximate free surface influences for various free surface geometries. Because of the limited accuracy and limited number of possible three-dimensional comparisons, estimates of the interaction between the free surface and stress distribution for three-dimensional cracks can be ^{assisted} assigned for specific problems and on an individual basis, by comparison to known two-dimensional results.

1. TWO-DIMENSIONAL EDGE CRACK PROBLEMS

As was discussed in the introduction, when surface cracks have a large surface length-to-depth ratio, solutions for two-dimensional edge crack problems provide approximate stress intensity factors for the region near the deepest crack edge.

One of the objectives of this section would be to provide information about free surface effects on stress intensity factors in two-dimensional crack problems. Some useful solutions for various geometric and loading configurations are illustrated.

A. An Edge Crack in Half-Plane (Straight Free Boundary)

Figure 1a.

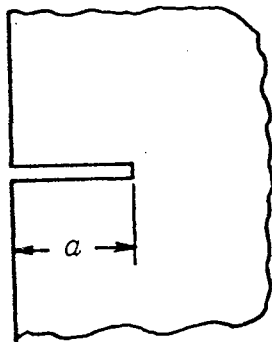


Figure 1a

Stress intensity factors for various loading conditions are known for this geometry. Only approximate formulae and their estimated accuracies will be presented for several basic stress distributions. For more information see Ref. 4, pp. 8.1-8.8.

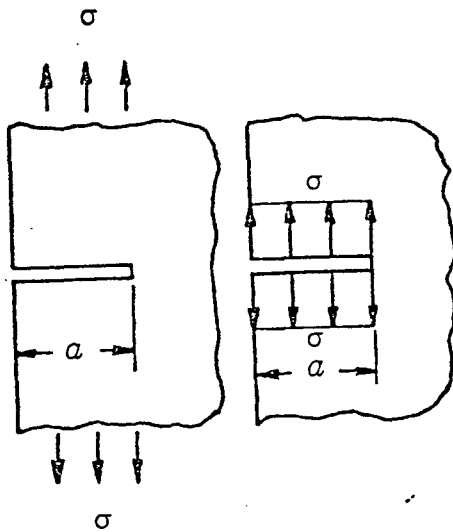


Figure 1b

(A-1) Uniform Tension, Fig. 1b.

$$K = 1.122 \sigma \sqrt{\pi a} \quad (1)$$

(accurate)

The factor representing free surface influence is 1.122.

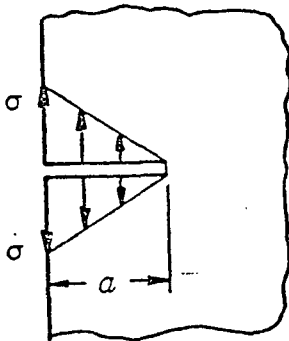


Figure 1c

(A-2) Linearly Varying Stress

(In-Plane Bending), Fig. 1c.

$$\left. \begin{aligned} K &= 0.439 \sigma \sqrt{\pi a} \\ &= 1.210 \left(1 - \frac{2}{\pi}\right) \sigma \sqrt{\pi a} \end{aligned} \right\} (2)$$

(accurate)

The factor representing free surface influences is 1.210.

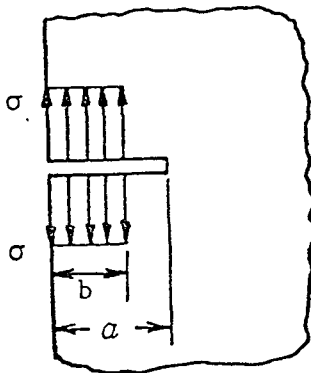


Figure 1d

(A-3) Partially Distributed Constant Pressure, Fig. 1d.

$$K = \frac{2}{\pi} \sigma \sqrt{\pi a} \left(\sin^{-1} \frac{b}{a}\right) F\left(\frac{b}{a}\right) \quad (3)$$

$$F\left(\frac{b}{a}\right) \simeq 1.30 - 0.18 \left(\frac{b}{a}\right)^{5/2}$$

(Better than 2% for any b/a)

F(b/a) is the free surface correction factor.

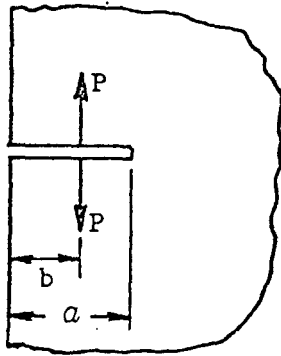


Figure 1e

(A-4) Concentrated Splitting Forces

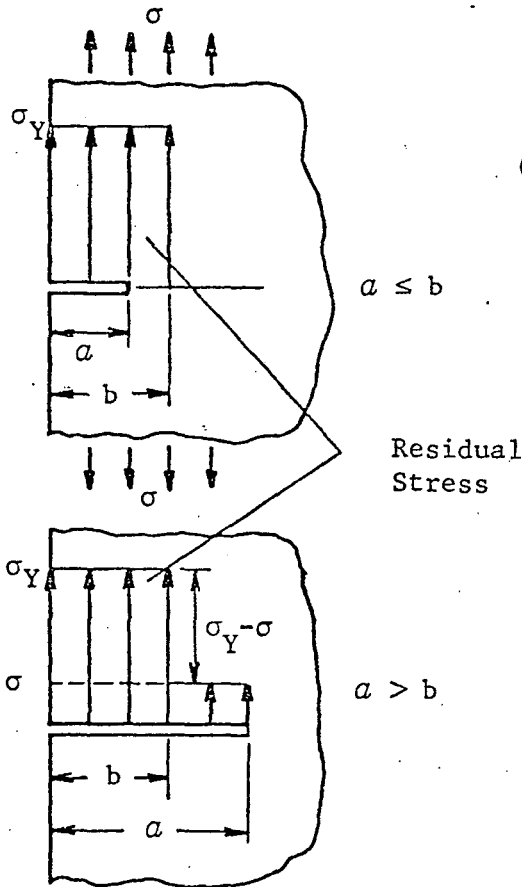
(Green's Function), Fig. 1e.

$$K = \frac{2P}{\sqrt{\pi a}} \frac{1}{\sqrt{1 - \left(\frac{b}{a}\right)^2}} \cdot F\left(\frac{b}{a}\right) \quad (4)$$

$$F\left(\frac{b}{a}\right) \approx 1.30 - 0.30 \left(\frac{b}{a}\right)^{3/2}$$

(Better than 2% for any b/a)

$F(b/a)$ is the free surface correction factor.



(A-5) Example:

Consider a crack extending through a tensile residual stress field (equal to yield stress σ_Y) under uniform tension, as shown in Fig. 1f.

When $a \leq b$, from Equation (1)

$$K = 1.122 \sigma_Y \sqrt{\pi a} \quad (5)$$

When $a > b$, from Equations

(1) and (3),

$$K = 1.122 \sigma \sqrt{\pi a} + \frac{2}{\pi} (\sigma_Y - \sigma) \sqrt{\pi a} \left(\sin^{-1} \frac{b}{a} \right) F\left(\frac{b}{a}\right) \quad (6)$$

Where $F(b/a)$ is given by Equation (3).

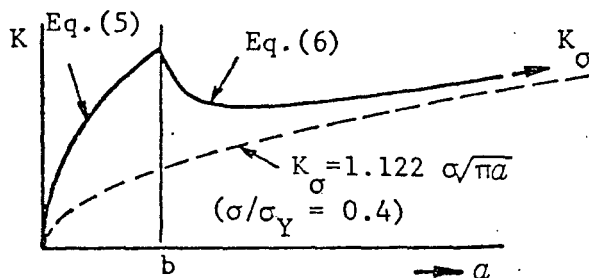


Figure 1f

Note:

1. For any non-uniform stress distributions, stress intensity factors are obtained by integration of Equation (4).
2. Equation (4) shows that the correction factor for a single free surface

$$K/K_{\infty} \leq 1.30 \quad (7)$$

for any normal stress distribution as long as the normal stress has the same sign over the entire crack length.

K_{∞} is the solution for the infinite plane with geometry and loading configuration reflected across the free boundary, Fig. 2.

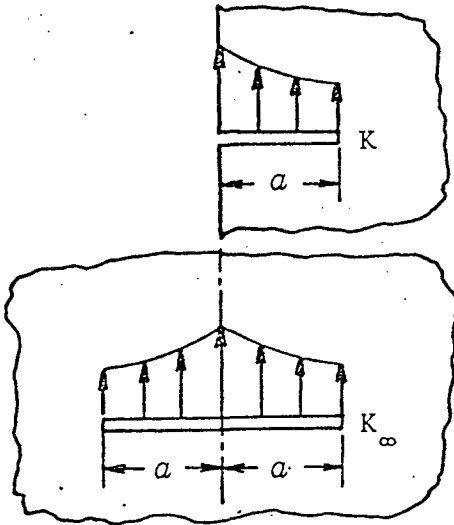


Figure 2

For the infinite plane problem, the exact Green's function is known (in Eq.(4), $F(b/a) = 1$) and K_{∞} calculations are considerably simpler.

3. In engineering practice, when only the rough idea with acceptable accuracy will suffice, one can simply estimate K as

$$K \sim 1.15 K_{\infty} \quad (8)$$

without causing substantial error. The error is never beyond 15% and usually much less. (When the normal stress has the same sign over the entire crack.) A complicated, more rigorous analysis may not be justified.

4. When a more accurate value is desirable, K estimate is improved by separating non-uniform stress into uniform stress and non-uniform stress as shown in Fig. 4.

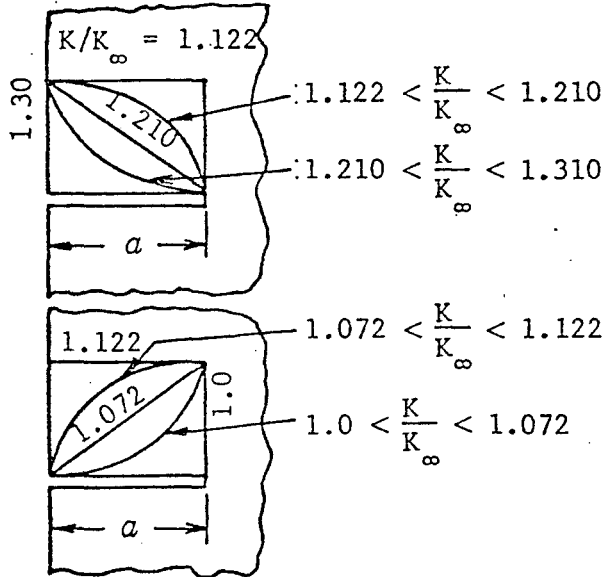


Figure 3

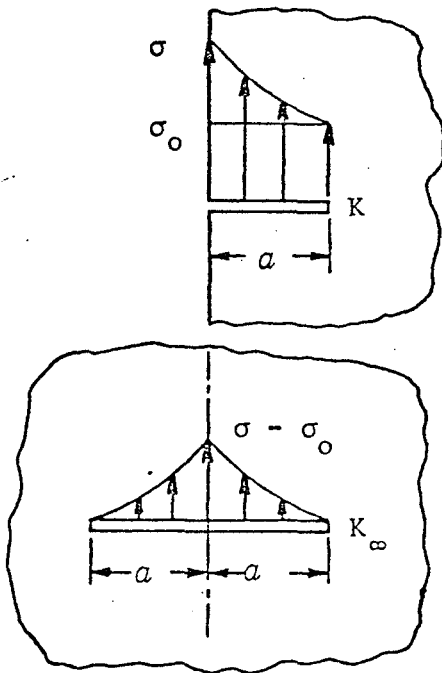


Figure 4

From Equations (1) through (4), the ranges of free surface correction factors K/K_∞ for various non-uniform stress distributions are known (Figure 3) and the values at the middle of the range are within 4% accuracy. For the example shown in Figure 4, K is estimated as

$$K \approx 1.122 \sigma_0 \sqrt{\pi a} + 1.255 K_\infty \quad (9)$$

and the accuracy improves as σ_0/σ increases. (Even when $\sigma_0 = 0$, accuracy is within 4%).

Although this method applies to the case where the stress distribution changes its sign over the crack length, the accuracy is not expected to be as good.

B. An Edge Crack in Half-Plane (Free Boundary Consists of Two Straight Lines), Figure 6a.

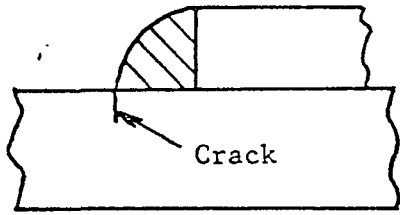


Figure 5

In welded structures or components, surface cracks often initiate in the residual stress zone near the welding as shown in Figure 5. When the crack is relatively small, the solutions for the configuration shown in Figure 6 may have some value for estimating stress intensity factors.

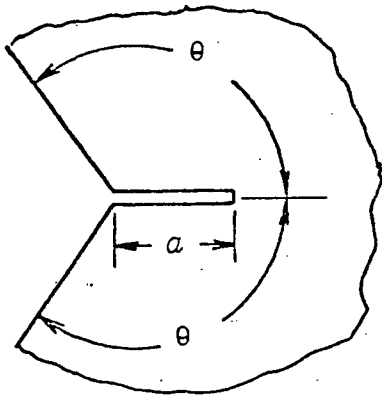


Figure 6a

Approximate formulas for stress intensity factors and their estimated accuracies are given for several loading conditions. These formulas were established based on an interpolation method.

(B-1) Uniform Normal Stress, Figure 6b.

$$K = \sigma \sqrt{\pi a} F(S)$$

$$F(S) = \frac{0.175 + 0.266S + 0.373S^2 + 0.126S^3}{S^{3/2}} \quad (10)$$

(Better than 1% for any S)

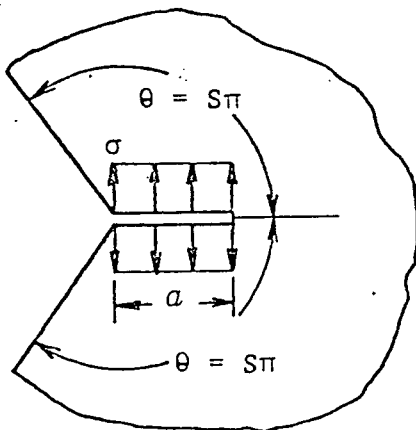


Figure 6b

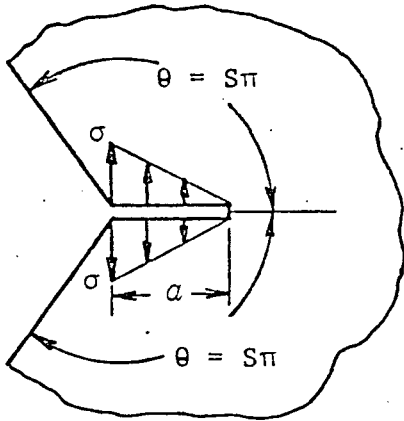


Figure 6c

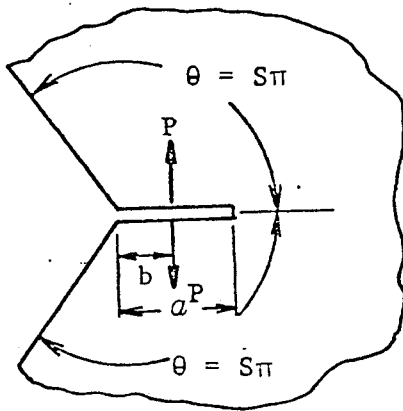


Figure 6d

(B-2) Linearly Varying Stress (In-Plane Bending), Figure 6c.

$$K = \sigma \sqrt{\pi a} F(S)$$

$$F(S) = \frac{0.117 + 0.022S + 0.055S^2 + 0.106S^3}{S^{3/2}} \quad (11)$$

(Better than 1% for any S)

(B-3) Concentrated Splitting Forces (Green's Function), Figure 6d.

$$K = \frac{P}{\sqrt{\pi(a-b)}} \cdot F\left(\frac{b}{a}, S\right)$$

$$F\left(\frac{b}{a}, S\right) = \frac{A + BS + CS^2 + DS^3}{S^{3/2}} \quad (12)$$

$$A = f(b/a)$$

$$B = -3.54 - 4f(b/a) + g(b/a)$$

$$C = 9.19 + 5f(b/a) - 2g(b/a)$$

$$D = -4.24 - 2f(b/a) + g(b/a)$$

$$f(b/a) = 1.10 (1 - b/a)^{3/2}$$

$$g(b/a) = \frac{+7.35 - 1.70(b/a)^{3/2}}{\sqrt{1 + b/a}}$$

(Much better than 5%; better than 2% for $S \geq 0.5$)

When $b = 0$

$$F(0, S) = \frac{1.10 - 0.60S + 0.03S^2 + 0.89S^3}{S^{3/2}} \quad (12a)$$

(Better than 2% for any S)

C. An Edge Crack in a Long Strip, Figure 7a.

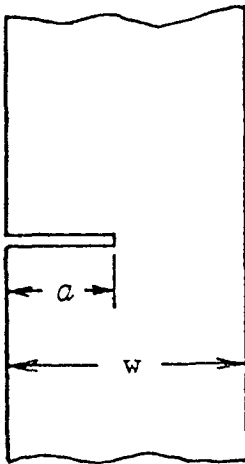


Figure 7a

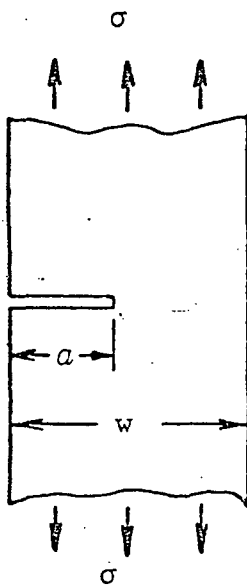


Figure 7b

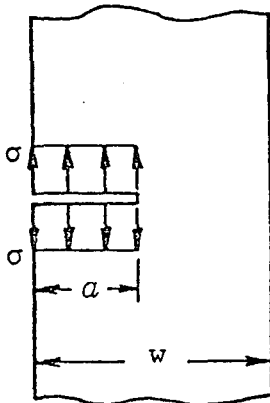


Figure 7c

Stress intensity factor solutions are known for various loading conditions for this geometry. Only approximate formulas and their accuracies are given for several basic cases. For more information see Ref. 4, pp. 2.10 - 2.21 and 2.25 - 2.29.

(C-1) Uniform Tension, Figures 7b, 7c

$$K = \sigma \sqrt{\pi a} F(a/w)$$

$$F(a/w) = \sqrt{\frac{2w}{\pi a} \tan \frac{\pi a}{2w}}$$

$$\times \frac{0.752 + 2.02 \frac{a}{w} + 0.37(1 - \sin \frac{\pi a}{2w})^3}{\cos \frac{\pi a}{2w}} \quad (13)$$

(Better than 0.5% for any a/w)

(C-2) Uniform Bending, Figure 7d

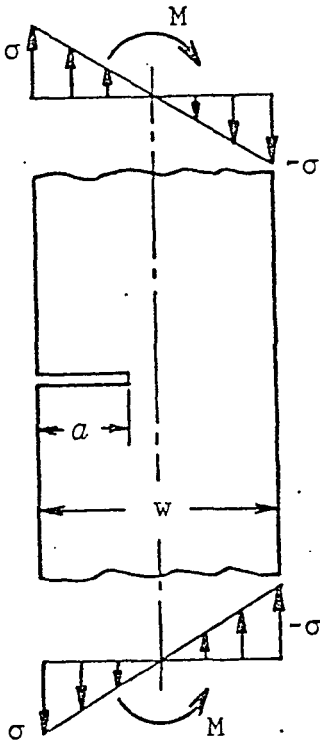


Figure 7d

$$\sigma = \frac{6 M}{b^2}$$

$$K = \sigma \sqrt{\pi a} : F(a/w) \quad (14)$$

$$F(a/w) = \sqrt{\frac{2w}{\pi a} \tan \frac{\pi a}{2w}}$$

$$\times \frac{0.923 + 0.199 (1 - \sin \frac{\pi a}{2w})^4}{\cos \frac{\pi a}{2w}}$$

(Better than 0.5% for any a/w)

(C-3) Concentrated Splitting Forces
(Green's Function), Figure 7e

$$K = \frac{2P}{\sqrt{\pi a}} F(b/a, a/w)$$

$$F(b/a, a/w) = \frac{3.52 (1 - b/a)}{(1 - a/w)^{3/2}}$$

$$- \frac{4.35 - 5.28 b/a}{(1 - a/w)^{1/2}}$$

$$+ \left\{ \frac{1.30 - 0.30 (b/a)^{3/2}}{\sqrt{1 - (b/a)^2}} \right.$$

$$\left. + 0.83 - 1.76 b/a \right\} \left\{ 1 - (1 - b/a) a/w \right\}$$

(15)

(Better than 2% for any b/a and a/w)

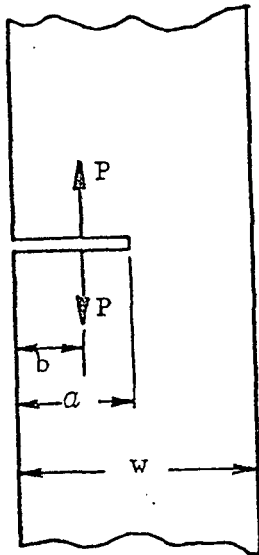


Figure 7e

(C-4) Example:

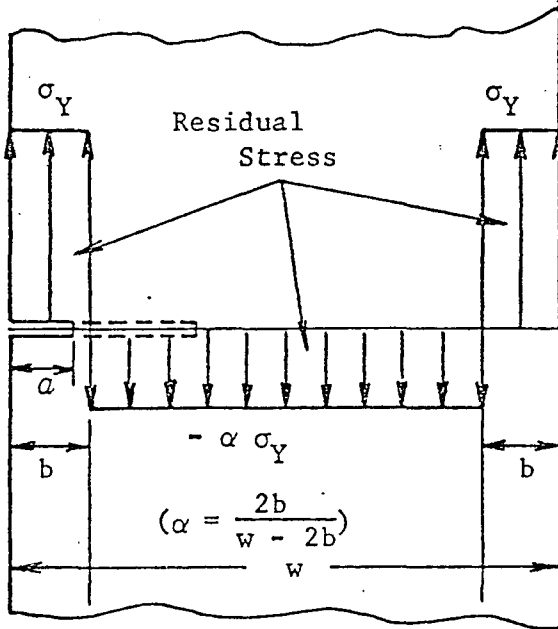


Figure 8a

Consider an edge crack extending in a residual stress field, as shown in Figure 8a.

$$\left(\frac{b}{w} = \frac{1}{7}; \quad \alpha = \frac{2}{5}\right)$$

When $a \leq b$

$$K = \sigma_Y \sqrt{\pi a} \quad F(a/w) \quad (16)$$

When $b \leq a (< w - b)$

$$K = (1+\alpha) \sigma_Y \sqrt{\pi a} F_1(b/a, a/w) - \alpha \sigma_Y \sqrt{\pi a} F(a/w) \quad (17)$$

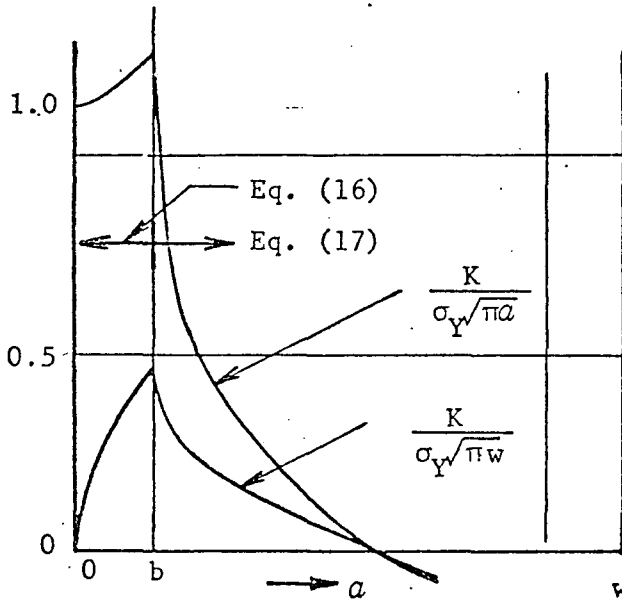


Figure 8b

In Figure 8b, numerical values of Equations (16) and (17) are plotted. It is noticed that the value of the stress intensity factor rapidly decreases as the crack extends beyond the tensile residual stress zone.

Where $F(a/w)$ is given by

Equation (13) and $F_1(b/a, a/w)$ is free surface correction for the uniform pressure distributed on a portion of the crack.

Numerical values of $F_1(b/a, a/w)$ up to $a/w \sim 0.62$ are read from the curves given by Emery, et al.⁵ (Figure 3 in Ref. 5)

$a \geq w - b$ is not considered.

It should be noted that the solutions illustrated above are valid only when the displacement of the strip is free from constraint. In actual structures, any connected structural member is under constraints imposed by the connections. When a crack occurs in a certain component, its compliance increases and load and deformation are redistributed between members. Thus, the boundary condition is not displacement-free but displacement-limited. If the change in compliance of the cracked member is known as a function of the crack size, such statically indeterminate problems will be solved by usual methods of structure analysis. The fracture mechanics method is helpful to establish the relationship between compliance and crack size of the component.

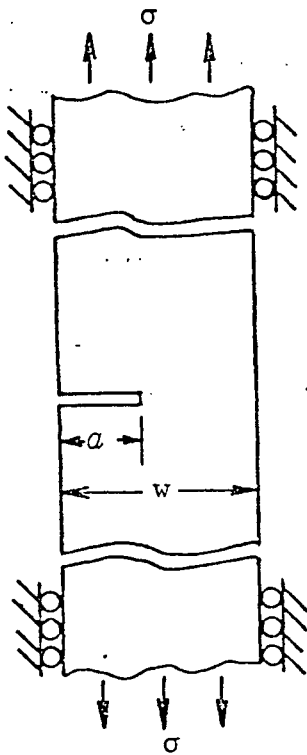


Figure 9a

(C-5) Examples of displacement constrained strip with a single edge crack are given in Figure 9. The in-plane transverse displacement at infinity is restrained.

The stress intensity factors are given by the following formulas

$$K = \sigma \sqrt{\pi a} F(a/w)$$

Where:

- a. When the local in-plane transverse displacement near the cracked section is not restrained (Figure 9a)

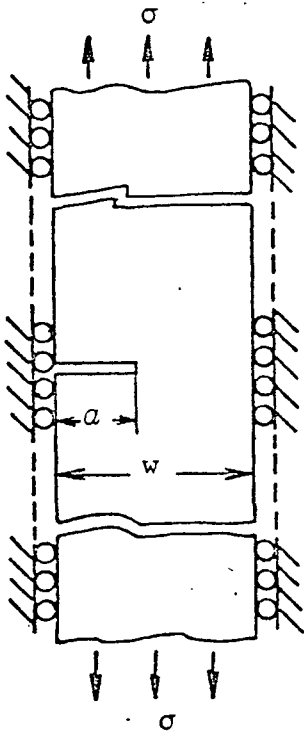


Figure 9b

Equation (18) is 12 to 30 percent larger than Equation (19). When the strip has attachments such as stiffeners, Equation (19) is expected to give reasonable estimates for stress intensity factors. An edge crack in the flange plate of a beam is a typical example in practical structures.

$$F\left(\frac{a}{w}\right) = \frac{1.122 - 0.561 \frac{a}{w} + 0.085 \left(\frac{a}{w}\right)^2 + 0.180 \left(\frac{a}{w}\right)^3}{\sqrt{1 - \frac{a}{w}}} \quad (18)$$

(Better than 2% for any a/w)

- b. When the local transverse displacement is also restrained (Figure 9b)

$$F\left(\frac{a}{w}\right) = \sqrt{\frac{2w}{\pi a} \tan \frac{\pi a}{2w}} \quad (19)$$

(Exact)

2. THE HALF-CIRCLE AND QUARTER-CIRCLE SURFACE CRACKS

A. A Circular Crack in an Infinite Body

Corresponding to a policy of treating the influence of free surfaces as a superimposed correction factor (see Section 1A), the K calculations for surface cracks of half-circle and quarter-circle shape depend in a basic way upon the K values for a circular (penny-shaped) crack in an infinite body subjected to various normal stress distributions.

(A-1) When the normal stress distributions have circular symmetry, the K is independent of position along the crack border. Furthermore, the analytical simplicity thus obtained permits computation of K for any normal stress distribution, $p(r)$, from the following equation.

$$K = \int_0^a p(r) f(r) dr \quad (20)$$
$$f(r) = \frac{2}{\sqrt{\pi a}} \frac{r}{\sqrt{a^2 - r^2}}$$

where a is the radius of the circular crack.

Results for a number of such stress distributions are given in Reference 4.

(A-2) When the normal stress distributions are not circular, the stress intensity factor which is dependent on position along the crack border can be calculated using the solution for concentrated splitting force problems.

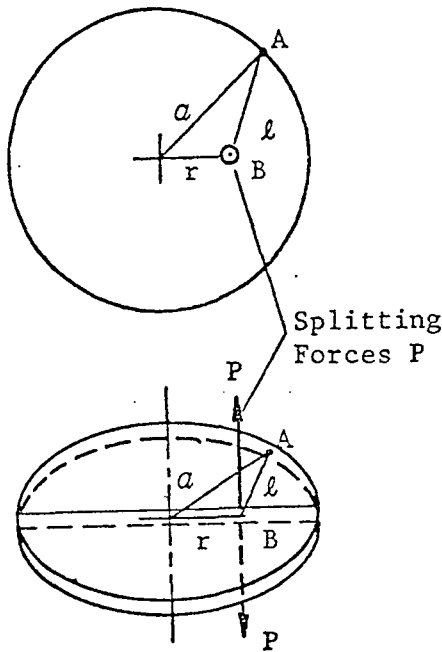


Figure 10

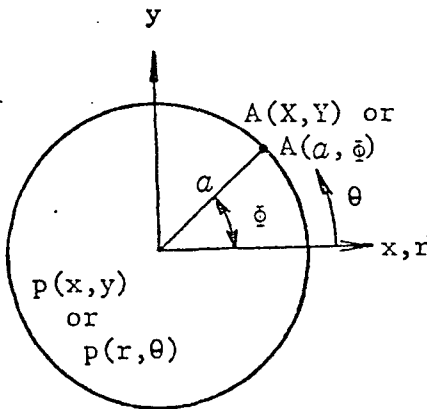


Figure 11

When a pair of splitting forces P are applied at point B , the stress intensity factor at point A (see Figure 10) is given by (4)

$$K = \frac{P}{\pi\sqrt{\pi a}} \frac{\sqrt{a^2 - r^2}}{l^2} \quad (21)$$

For any normal stress distribution $p(x, y)$ or $p(r, \theta)$, the stress intensity factor at point A , $K(X, Y)$ or $K(\bar{\theta})$, is calculated by Equation (21) as follows (see Figure 11)

$$K(X, Y) = \iint p(x, y) f_1(X, Y; x, y) dx dy$$

over
 $x^2 + y^2 \leq a^2$

(22a)

where

$$f_1(X, Y; x, y) = \frac{1}{\pi\sqrt{\pi a}} \frac{\sqrt{a^2 - x^2 - y^2}}{(X-x)^2 + (Y-y)^2}$$

or

$$K(\bar{\theta}) = \int_{r=0}^a \int_{\theta=0}^{2\pi} p(r, \theta) f_2(\bar{\theta}; r, \theta) r d\theta dr$$

where

$$f_2(\bar{\theta}; r, \theta) = \frac{1}{\pi\sqrt{\pi a}} \frac{\sqrt{a^2 - r^2}}{a^2 + r^2 - 2ar \cos(\bar{\theta} - \theta)}$$

(22b)

Some examples are given in Ref. 4.

(A-3) Two-dimensional normal stress fields, $p(x,y) = p(y)$, such as uniform bending field are special cases of (A-2). To analyze

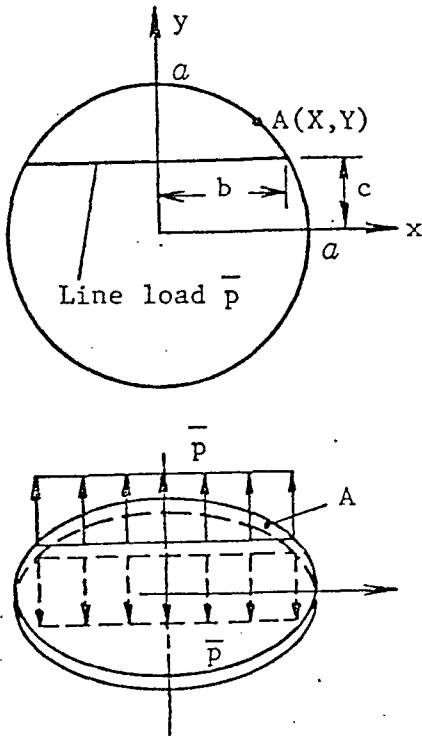


Figure 12

problems of this type, it is helpful to establish the solution for constant line load problem, Figure 12. When a constant line load \bar{p} is applied along $y = c$, the stress intensity factor at A, $K(X,Y)$ is calculated from Equation (21) or (22) as follows, see Figure 12.

$$K(X,Y) = \frac{\bar{p}}{\pi\sqrt{\pi a}} \int_{-b}^b \frac{\sqrt{b^2 - x^2}}{(X-x)^2 + (Y-c)^2} dx \quad (23)$$

where $b = \sqrt{a^2 - c^2}$

Equation (23) is reduced to the following simple form

$$K(X,Y) = \frac{\bar{p}}{\sqrt{\pi a}} \left(\sqrt{\frac{l_2}{l_1}} - 1 \right) \quad (24)$$

or

$$K(X,Y) = \frac{\bar{p}}{\sqrt{\pi a}} \left(\sqrt{\frac{a+Y}{Y-c}} - 1 \right) \text{ when } Y > c$$

$$K(X,Y) = \frac{\bar{p}}{\sqrt{\pi a}} \left(\sqrt{\frac{a-Y}{c-Y}} - 1 \right) \text{ when } Y < c \quad (25)$$

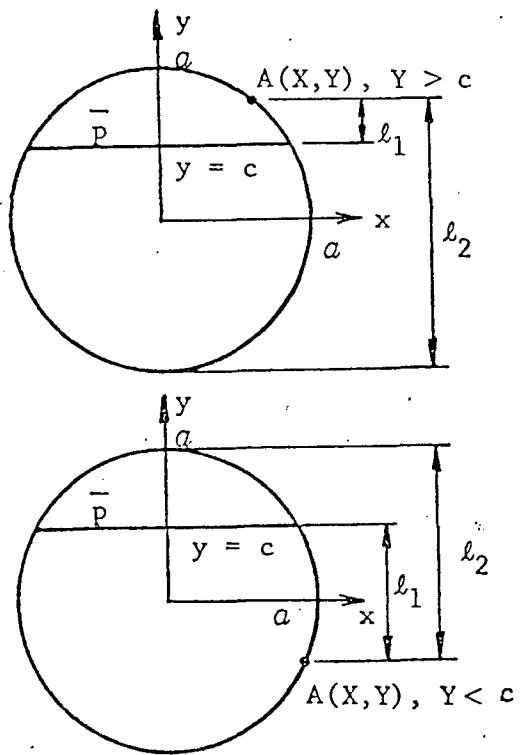


Figure 13

See Figure 13.

The stress intensity factors for any two-dimensional normal stress distributions, $p(y)$, are calculated by Equation (25) as follows:

$$K(X,Y) = \int_{-a}^Y p(y) f_1(y,Y) dy + \int_Y^a p(y) f_2(y,Y) dy \quad (26)$$

where

$$f_1(y,Y) = \frac{1}{\sqrt{\pi a}} \left(\sqrt{\frac{a+Y}{Y-y}} - 1 \right)$$

$$f_2(y,Y) = \frac{1}{\sqrt{\pi a}} \left(\sqrt{\frac{a-Y}{y-Y}} - 1 \right)$$

For an example, the stress intensity factor at point A, for a "tent-shaped" two-dimensional normal stress distribution $p(y) = p(1 - \frac{|y|}{a})$

as shown in Figure 14, is calculated by Equation (26).

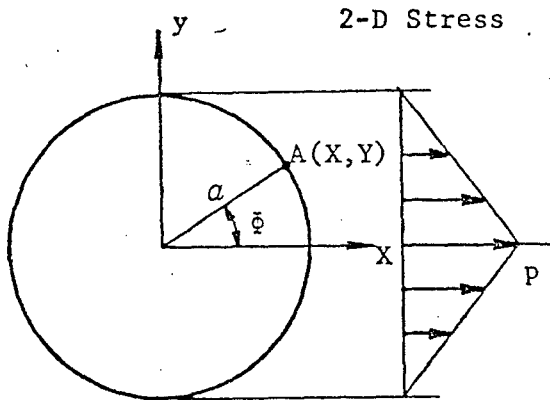


Figure 14

$$K(X,Y) = \int_{-a}^Y \left(1 - \frac{|y|}{a}\right) f_1(y,Y) dy + \int_Y^a \left(1 - \frac{|y|}{a}\right) f_2(y,Y) dy$$

For $Y > 0$

$$= \int_{-a}^0 \left(1 + \frac{y}{a}\right) f_1(y,Y) dy + \int_0^Y \left(1 - \frac{y}{a}\right) f_1(y,Y) dy + \int_Y^a \left(1 - \frac{y}{a}\right) f_2(y,Y) dy$$

The final expression is

$$K(X,Y) = \frac{2}{\pi} p \sqrt{\pi a} \left\{ \frac{5}{6} - \frac{4}{3} \left(\frac{Y}{a}\right)^{3/2} \left(\sqrt{1 + \frac{Y}{a}} - \sqrt{\frac{Y}{a}} \right) \right\} \quad (27a)$$

or

$$K(\phi) = \frac{2}{\pi} p \sqrt{\pi a} \left\{ \frac{5}{6} - \frac{4}{3} (\sin \phi)^{3/2} \left(\sqrt{1 + \sin \phi} - \sqrt{\sin \phi} \right) \right\} \quad (27b)$$

K is symmetric with respect to x axis ($y = 0$). This is the exact solution of the problem and $K(\phi)$ is plotted in Figure 18.

B. The Half-Circle Surface Crack and the Quarter-Circle Corner Crack

For a half-circle surface crack and a quarter-circle corner crack, the influences of free surfaces are treated as corrections to the solution for the circular crack with the normal stress distribution reflected across the free surfaces. The free surface corrections are defined in Figure 15.

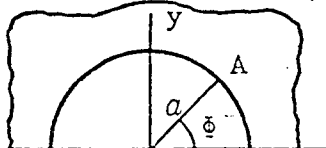
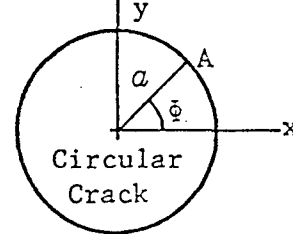
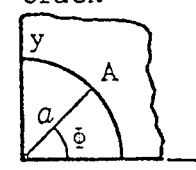
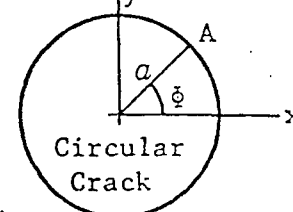
Crack Geometry	Normal Stress Distribution	Stress Intensity Factor at A	Free Surface Correction Factor
<p>Half-Circular Surface Crack</p> 	$p(x,y) = f(x,y)$	$K_H(\phi) = K_0(\phi) \cdot F_H(\phi)$	$F_H(\phi)$
<p>Circular Crack</p> 	$p(x,y) = f(x, y)$	$K_0(\phi)$	
<p>Quarter-Circular Corner Crack</p> 	$p(x,y) = f(x,y)$	$K_Q(\phi) = K_0(\phi) \cdot F_Q(\phi)$	$F_Q(\phi)$
<p>Circular Crack</p> 	$p(x,y) = f(x , y)$	$K_0(\phi)$	--

Figure 15

Discussions will be made for the following two cases where the exact solutions for the circular crack, $K_0(\phi)$, and the numerical values for the half-circle crack, $K_H(\phi)$, and the quarter-circle crack, $K_Q(\phi)$, are available.

(1) Uniform Tension

(2) Linearly Varying Stress

Approximate formulas for free surface correction factors will be presented for these cases.

(B-1) Uniform Tension $p(x,y) = \sigma$

For a circular crack, the exact solution is

$$K_0(\phi) = \frac{2}{\pi} \sigma \sqrt{\pi a} \quad (28)$$

For a half-circle surface crack, an approximate formula for the free surface correction factor, $F_H(\phi)$ is available.

$$K_H(\phi) = \frac{2}{\pi} \sigma \sqrt{\pi a} F_H(\phi) \quad (29)$$

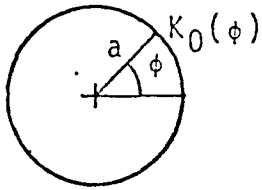
where

$$F_H(\phi) = 1.211 - 0.186 \sqrt{\sin \phi} \\ (\phi > 10^\circ)$$

This $F_H(\phi)$ formula was obtained by Merkle² based on the analytical results by F. W. Smith et al⁶. $F_H(\phi)$ is shown in Figure 16.

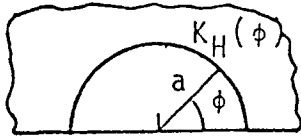
For a quarter-circle corner crack, there are Tracy's numerical result by a finite element method⁷ and the result of Kobayashi et al⁸ by the alternating procedure. There is some discrepancy between these results. Since Kobayashi et al

Uniform Tension σ



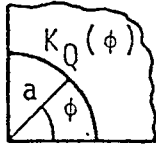
Circular Crack

$$K_0(\phi) = \frac{2}{\pi} \sigma \sqrt{\pi a}$$



Half-Circular Surface Crack

$$K_H(\phi) = \frac{2}{\pi} \sigma \sqrt{\pi a} \cdot F_H(\phi)$$



Quarter-Circular Corner Crack

$$K_Q(\phi) = \frac{2}{\pi} \sigma \sqrt{\pi a} \cdot F_Q(\phi)$$

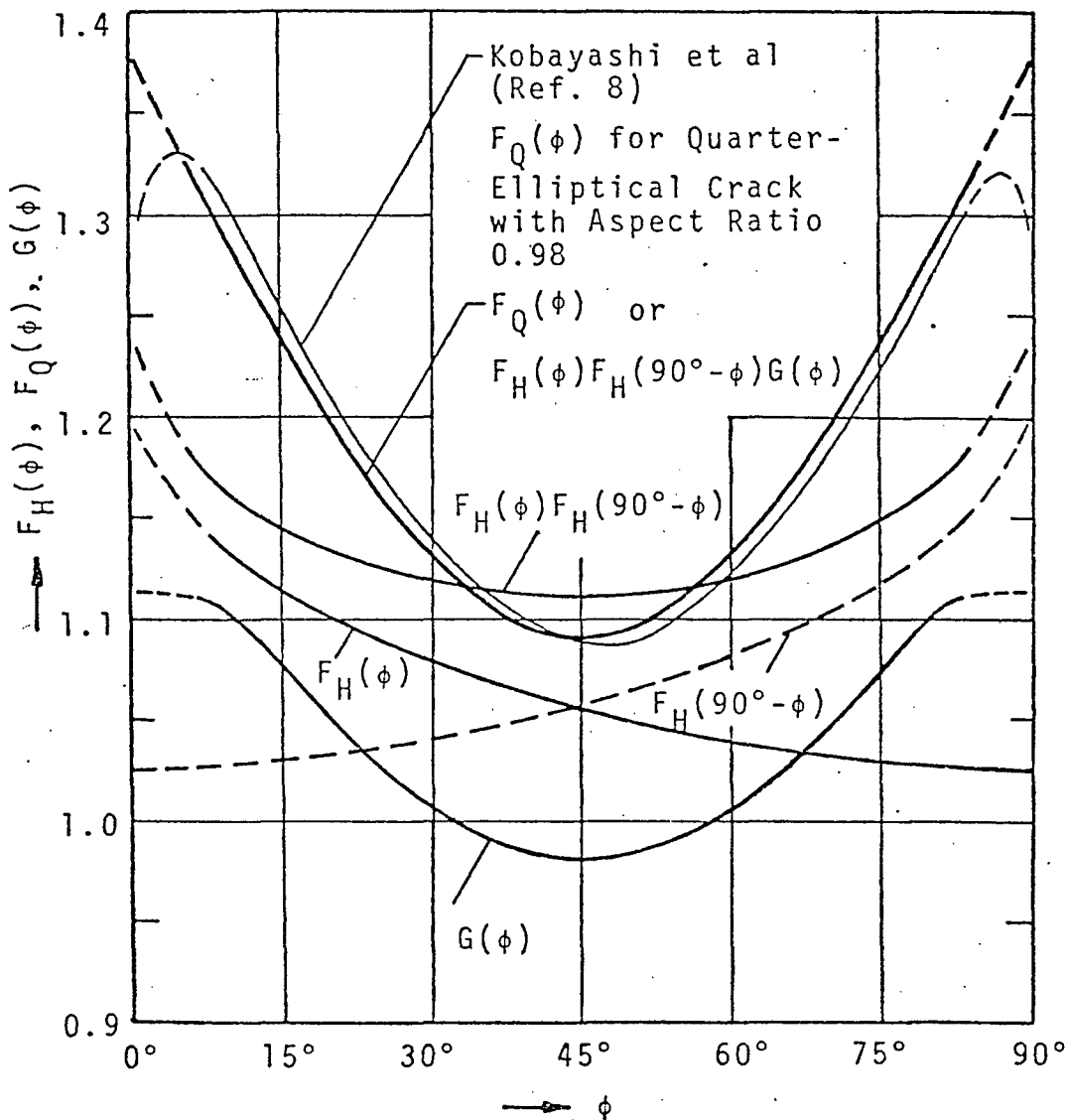


Figure 16 Free Surface Correction Factors for Half-Circular Surface Crack and Quarter-Circular Corner Crack Under Uniform Tension

estimated the accuracy of their result at better than 2%, except for the regions of the crack border near the free surfaces, their result is used as $K_Q(\phi)$. The crack shape in their analysis is slightly different from a quarter-circle (a quarter-elliptical crack with aspect ratio of 0.98), therefore their result was adjusted slightly. An approximate formula is given by

$$K_Q(\phi) = \frac{2}{\pi} \sigma \sqrt{\pi a} F_Q(\phi) \quad (30)$$

where

$$F_Q(\phi) = 1.38 - 0.29 \sin 2\phi \\ (10^\circ < \phi < 80^\circ)$$

$F_Q(\phi)$ is shown in Figure 16.

In Figure 16, the values of the product of the correction factor to the half-circle for each surfaces $F_H(\phi) \cdot F_H(90^\circ - \phi)$ are also shown for comparison. It is suggested that the free surface correction to a corner crack is not given by the product of the correction factor for each surface, but given by the following form

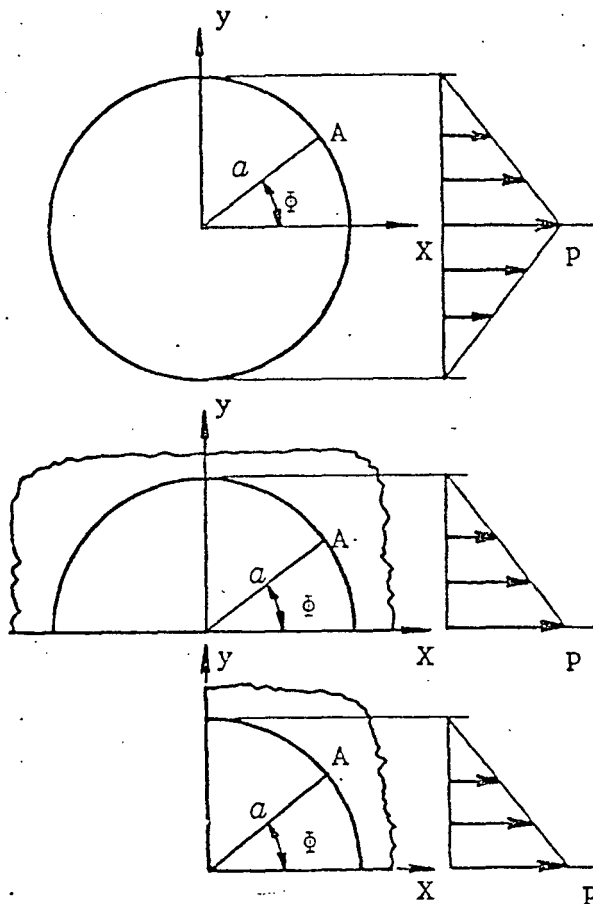
$$F_Q(\phi) = F_H(\phi) F_H(90^\circ - \phi) \cdot G(\phi) \quad (31)$$

For a special case of uniform tension $G(\phi)$ is approximately given by the formula

$$G(\phi) = 1.17 - 0.19 \sin 2\phi \\ (10^\circ < \phi < 80^\circ) \quad (32)$$

However, in the middle region of the crack border ($25^\circ < \phi < 65^\circ$), the difference between $F_Q(\phi)$ and $F_H(\phi) F_H(90^\circ - \phi)$ is within 2%.

(B-2) Linearly Varying Stress: $p(x,y) = p \left(1 - \frac{|y|}{a}\right)$



The stress intensity factor in the bending stress field for the half-circular surface crack and the quarter-circular corner can be discussed by the solution for the linearly varying two-dimensional normal stress distributions shown in Figure 17.

For the circular crack, the exact stress intensity factor is given by Equation (27).

Figure 17

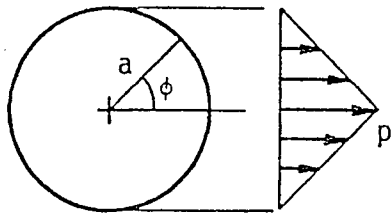
$$K_0(\phi) = \frac{2}{\pi} p \sqrt{\pi a} f_0(\phi) \quad (33)$$

where

$$f_0(\phi) = \frac{5}{6} - \frac{4}{3} (\sin \phi)^{3/2} \left(\sqrt{1 + \sin \phi} - \sqrt{\sin \phi} \right)$$

$f_0(\phi)$ is shown in Figure 18.

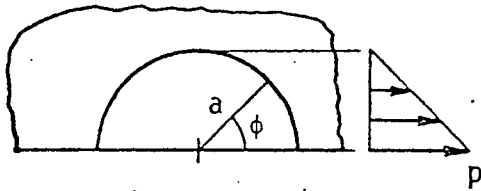
For the half-circular surface crack, there is an approximate formula given by Merkle² based on the results of F. W. Smith et al⁶, which is expressed as follows.



Circular Crack

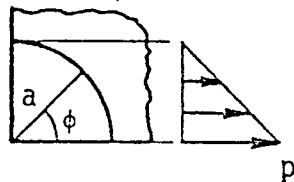
$$K_0(\phi) = \frac{2}{\pi} p \sqrt{\pi a} \cdot f_0(\phi)$$

$$f_0(\phi) = \frac{5}{6} - \frac{4}{3} (\sin \phi)^{3/2} (\sqrt{1 + \sin \phi} - \sqrt{\sin \phi})$$



Half-Circular Surface Crack

$$K_H(\phi) = \frac{2}{\pi} p \sqrt{\pi a} \cdot f_H(\phi)$$



Quarter-Circular Corner Crack

$$K_Q(\phi) = \frac{2}{\pi} p \sqrt{\pi a} \cdot f_Q(\phi)$$

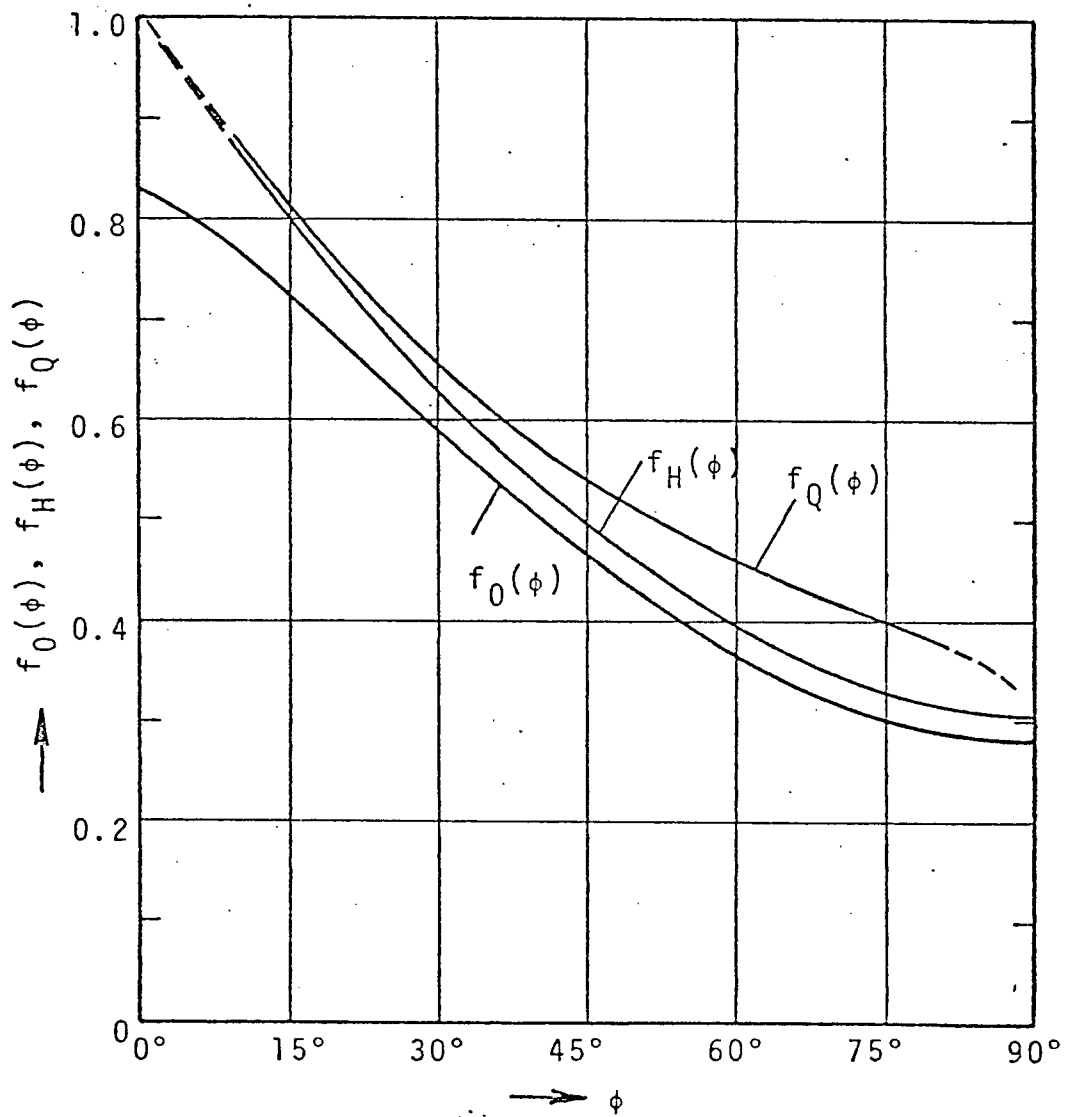


Figure 18 Stress Intensity Factors for Circular Crack, Half-Circular Surface Crack and Quarter-Circular Corner Crack Under Linearly Varying Stress Fields

$$K_H(\phi) = \frac{2}{\pi} p \sqrt{\pi a} f_H(\phi) \quad (34)$$

where

$$f_H(\phi) = 1.031 - 0.186 \sqrt{\sin \phi} - 0.54 \sin \phi \\ (10^\circ < \phi \leq 90^\circ)$$

$f_H(\phi)$ is shown in Figure 18.

For the quarter-circular corner crack, there is the result of Kobayashi et al by the alternating procedure⁸. Their result is approximated by the following formula

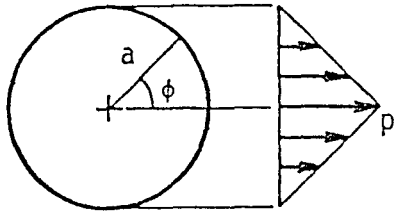
$$K_Q(\phi) = \frac{2}{\pi} p \sqrt{\pi a} f_Q(\phi) \quad (35)$$

where

$$f_Q(\phi) = 1 - 0.72 \sin \phi + 0.11 (\sin \phi)^2 \\ (10^\circ < \phi < 80^\circ)$$

$f_Q(\phi)$ obtained by Kobayashi et al is shown in Figure 18 and compared with the approximate formula Equation (35).

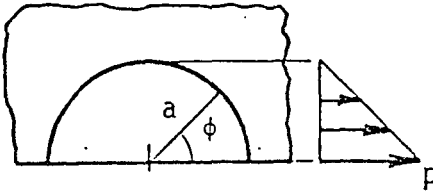
It is noted that Equations (34) and (35) are not expressed in terms of the free surface corrections. The free surface corrections are not $f_H(\phi)$ and $f_Q(\phi)$ but $F_H(\phi) = f_H(\phi)/f_0(\phi)$ and $F_Q(\phi) = f_Q(\phi)/f_0(\phi)$, respectively. It seems that no discussions have been made in terms of the free boundary corrections for the case of linearly varying normal stress distribution, because the exact solution for the circular crack under two-dimensional "tent-shaped" stress field, $f_0(\phi)$, had not been known.



Circular Crack

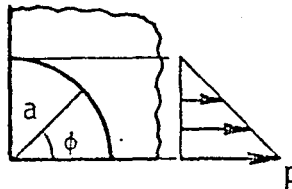
$$K_0(\phi) = \frac{2}{\pi} p \sqrt{\pi a} \cdot f_0(\phi)$$

$$f_0(\phi) = \frac{5}{6} - \frac{4}{3}(\sin\phi)^{3/2}(\sqrt{1+\sin\phi} - \sqrt{\sin\phi})$$



Half-Circular Surface Crack

$$K_H(\phi) = K_0(\phi) \cdot F_H(\phi)$$



Quarter-Circular Corner Crack

$$K_Q(\phi) = K_0(\phi) \cdot F_Q(\phi)$$

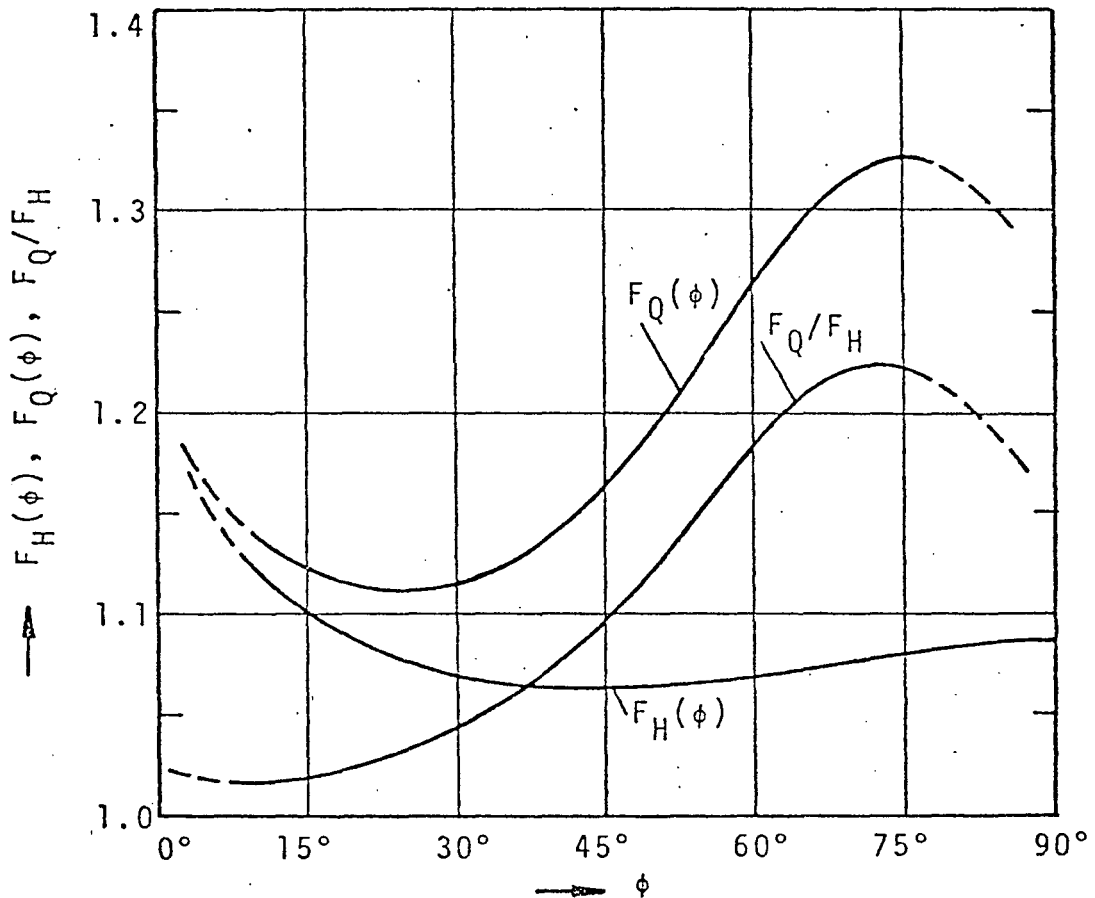


Figure 19 Free Surface Correction Factors for Half-Circular Surface Crack and Quarter-Circular Corner Crack Under Linearly Varying Stress Field

Since $f_0(\phi)$ is given by Equation (33) the surface correction factors $F_H(\phi)$ and $F_Q(\phi)$ are calculated. The values of $F_H(\phi)$ and $F_Q(\phi)$ are shown in Figure 19. The approximate formulas for $F_H(\phi)$ and $F_Q(\phi)$ are expressed as follows:

$$F_H(\phi) = 1.17 - 0.31 \sin \phi + 0.32 (\sin \phi)^2 \quad (36)$$

$$(10^\circ < \phi < \leq 90^\circ)$$

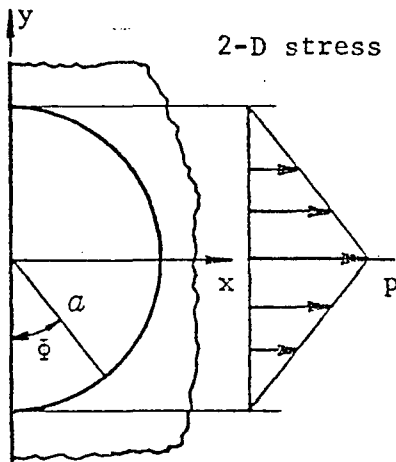
and

$$F_Q(\phi) = 1.22 - 0.56 \sin \phi + 0.70 (\sin \phi)^2 \quad (37)$$

$$(10^\circ < \phi < 80^\circ)$$

Corresponding to Equation (31), $F_Q(\phi)$ is expressed as the following product

$$F_Q(\phi) = F_H(\phi) \cdot F_H'(90^\circ - \phi) \cdot G(\phi) \quad (38)$$



$$K_H(\phi) = K_0(\phi) \cdot F_H'(\phi)$$

Figure 20

$$F_H'(90^\circ - \phi) \cdot G(\phi) = 1.03 - 0.17 \sin \phi + 0.39 (\sin \phi)^2$$

$$(10^\circ < \phi < 80^\circ)$$

(39)

where $F_H'(\phi)$ is the free surface correction factor for the circular crack shown in Figure 20. However, since $F_H'(\phi)$ is not known for this case $G(\phi)$ can not be separated. The curve for $F_H'(90^\circ - \phi) \cdot G(\phi) = F_Q(\phi)/F_H(\phi)$ is shown in Figure 19, which is approximated by the following formula.

(B-3) Estimates of Stress Intensity Factors for the Half-Circular Surface Crack and the Quarter-Circular Corner Crack under Arbitrary Two-Dimensional Normal Stress Distribution:

$$p(x,y) = p(y).$$

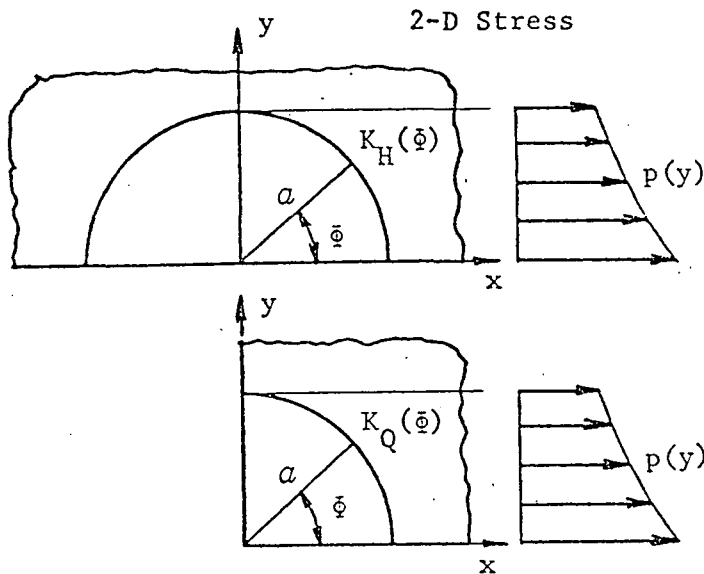


Figure 21

Any non-uniform stress distributions, $p(y)$, can be separated as

$$p(y) = p_0 + p_1(y) \quad (40)$$

where p_0 is uniform stress component and $p_1(y)$ is the non-uniform stress components as shown in Figure 22.

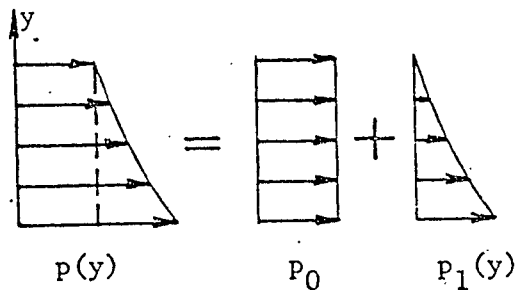


Figure 22

For the uniform stress component, the stress intensity factors for the half-circular and the quarter-circular cracks are given by Equations (29) and (30), respectively.

In engineering, when a rigorous analysis is not justified, the contribution of $p_1(y)$ to K values is reasonably estimated in the following way.

When the non-uniform stress component, $p_1(y)$, can be approximated by a linear stress distribution, the approximate K values are given by Equations (34) and (35), respectively. Thus the total stress intensity factors are obtained by superposition.

When $p_1(y)$ is not approximated by a linear stress field, the stress intensity factor for the circular crack, $K_0(\bar{\phi})$, under the normal stress distribution $p_1(|y|)$, Figure 23, is readily

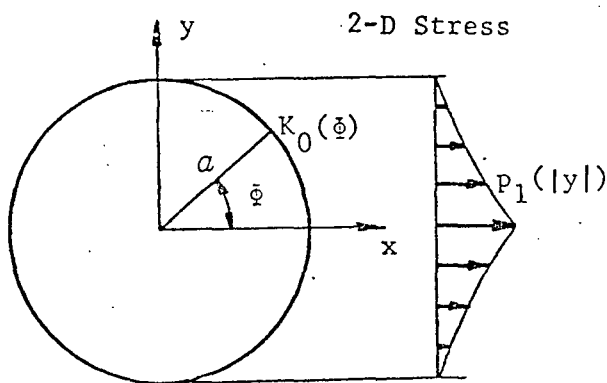


Figure 23

obtained by the simple integral, Equation (26), where $p(y) = p_1(|y|)$. Thus it is now only necessary to estimate the free surface corrections, $F_H(\bar{\phi})$ and $F_Q(\bar{\phi})$, for the stress field, $p_1(y)$.

From Figures 16 and 19, in the middle region of the crack border ($30^\circ \leq \bar{\phi} \leq 90^\circ$) for the half-circular surface crack and ($30^\circ \leq \bar{\phi} \leq 60^\circ$) for the quarter-circular corner crack), these correction factors are roughly

$$F_H(\bar{\phi}) \sim 1.05 \quad (41)$$

$$F_Q(\bar{\phi}) \sim 1.15 \quad (42)$$

Therefore the total stress intensity factors are estimated as follows:

For the half-circular surface crack

$$K_H(\phi) \simeq K_{HU}(\phi) + 1.05 K_0(\phi) \quad (43)$$
$$(30^\circ \leq \phi \leq 90^\circ)$$

and for the quarter-circular corner crack

$$K_Q(\phi) \simeq K_{QU}(\phi) + 1.15 K_0(\phi) \quad (44)$$
$$(30^\circ \leq \phi \leq 60^\circ)$$

where $K_{HU}(\phi)$ and $K_{QU}(\phi)$ are the K components for the uniform stress (given by Equations (29) and (30) with $\sigma = p_0$).

$K_0(\phi)$ is the stress intensity factor for the circular crack for the non-uniform stress component (given by Equation (26) with $p(y) = p_1(|y|)$).

Examinations of service fracture failures in which rapid fracturing started from a surface crack have rarely, if ever, shown evidence that the initial instability occurred close to a free surface. On the contrary, the fracture surface markings usually indicated that the instability was nearly simultaneous along a substantial segment of the internal (embedded) portion of the crack. It can be noted that the expected elevation of resistance to crack extension near the free surface would tend to offset the increase of K in such regions. Since the numerical calculations tend to lose accuracy near free surfaces, and in view of the primary region of instability suggested by fracture surface markings, an averaging of the numerical calculation of K across

a substantial portion of the deep region of the crack would be expected to provide the most appropriate value of K for purposes of comparison to K_{Ic} :

3. ELLIPTICAL SURFACE CRACKS

Methods of finite element analysis for three-dimensional cracks have been developed to a sufficient degree so that values of K for half or quarter elliptical surface cracks can be computed by this method with a potential accuracy of about 5 percent. However, this capability is localized and the calculations require substantial time and expense. In the case of cracks in welded bridge components, generally the residual stress from welding will contribute a large fraction of the total K for a crack and will be known with only limited accuracy. In addition, displacement constraint influences due to attachments are often present which are difficult to properly represent even in a sophisticated finite element K value computation. Thus methods of estimating K for elliptical surface cracks based on plausible engineering estimates seem most appropriate for this project.

It will be assumed that the trace of the leading edge of a surface crack can be represented as either one-quarter of an ellipse (for a crack extending from a corner region) or one-half of an ellipse. The methods of K value estimation to be ^{discussed} ~~desirable~~ will center attention first on the value of K which is applicable to the completely embedded crack disregarding free surfaces. The influences of free surfaces will be treated as correction factors.

Generally the part-through surface cracks which develop in welded steel bridge components occur in regions of metallurgical damage and

stress elevation due to welding. An engineer attempting to estimate the significant K value for such a crack must first establish a best judgment estimate of the normal stress across the plane of the crack which would be acting if the crack were not present. This will be termed the "crack-absent" distribution of tensile stress. In a real structure, estimation of the influence of residual stress due to welding on the crack-absent stress distribution can be assisted by study of reports of residual stress measurements across weldments of various kinds. In the interests of calculation simplicity and considering the uncertainties of estimates of welding residual stress, the influence of welding might be regarded as having elevated the stress to the level of the static tensile yield point of the material across a region comparable in size to the weldment. Outside of this region, although some allowance might be made for the balancing residual compressive stress, mainly the stress level would be that due ^{to} dead load and live load acting on the bridge structure component. This type of crack-absent stress pattern differs considerably from the non-uniform stress patterns which have received most attention in previous analysis of flat-elliptical cracks. The two K value estimation methods, termed A and B, discussed next appear to be suitable for the bridge component surface cracks of main interest in the current Lehigh DOT project. In method A, the crack-absent stress pattern must be regarded as having a special kind of symmetry relative to the elliptical contour of the crack. Method B is more general.

A. Method A

In the case of remote uniform tension, the K values around the perimeter of a flat-elliptical crack are well known. The equation is

$$K^2 = \frac{\sigma^2 \pi a}{E_k} \sqrt{1 - k^2 \cos^2 \bar{\phi}} \quad (45)$$

where E_k is the complete elliptic integral of the second kind, σ is the remote uniform tensile stress normal to the crack, and a is the smaller of the two semi-axes of the elliptical crack. The values of k and $\bar{\phi}$ are given as follows. Assume the boundary curve of the crack is given by the parametric equations, (see Figure 24).

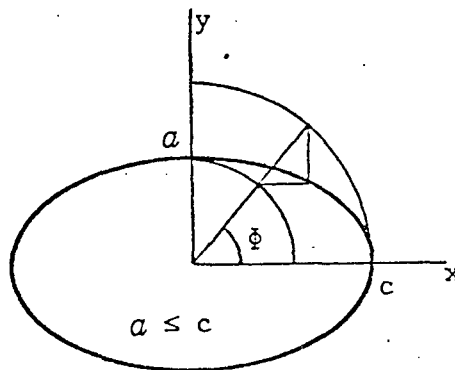


Figure 24

$$x = c \cos \bar{\phi}, \quad y = a \sin \bar{\phi} \quad (46)$$

where c is the major semi-axes. Thus c is equal to or larger than a . The Cartesian coordinate z is normal to the plane of the crack. k is defined by the equation

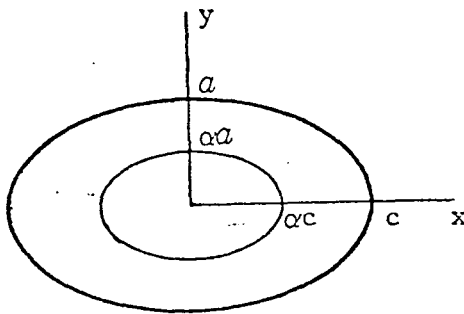
$$k^2 = 1 - (a/c)^2 \quad (47)$$

From the equation for E_k

$$E_k = \int_0^{\pi/2} \sqrt{1 - k^2 \cos^2 u} \, du \quad (48)$$

it can be seen that E_k approaches $\pi/2$ as c approaches a and k approaches zero, and that E_k approaches unity as a/c approaches zero and k approaches unity.

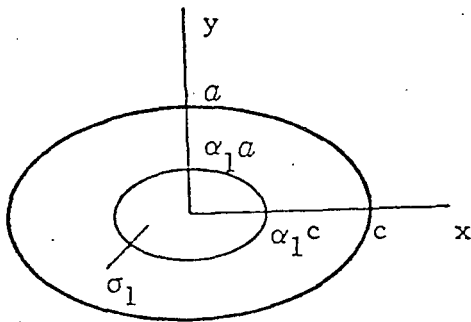
Assume next that the tension which would act across the plane of the crack, with the crack absent, is not uniform. Several service component situations are known for which it would be a reasonable approximation to assume that the stress σ_z , across the crack plane, which must be removed to establish free surfaces within the crack boundaries, is constant along the elliptical lines similar to the perimeter of the crack. These lines are defined by a parameter α as (see Figure 25).



$$\sigma_z = \sigma_z(\alpha)$$

$$0 \leq \alpha \leq 1$$

Figure 25



$$\sigma_z(\alpha) = \sigma_1$$

$$\alpha \leq \alpha_1$$

Figure 26

$$x = \alpha c \cos \phi, y = \alpha a \sin \phi \quad (49)$$

$$(0 \leq \alpha \leq 1)$$

As an approximation, the dependency of K upon ϕ can be assumed to be nearly the same as in Equation (45) when ϕ is in the range from 60° to 120° .

Assume next that σ_z has a certain constant value σ_1 within the elliptical line corresponding to $\alpha = \alpha_1$ in Equation (49), (See Figure 26). If $a = c$, then the K value is known to be given by the equation⁴

$$K^2 = \frac{4}{\pi} \sigma_1^2 a \{1 - \sqrt{1 - \alpha_1^2}\}^2 \quad (50)$$

as a/c approaches zero, the value of K near $\phi = 90^\circ$ (which is of main interest) is known to be given by⁴

$$K^2 = \frac{4}{\pi} \sigma_1^2 a \{\text{arc sin } \alpha_1\}^2 \quad (51)$$

A plausible approximation for values of a/c between unity and zero is given by the expression

$$K^2 = \frac{4}{\pi} \sigma_1 a \left[\left(\frac{a}{c}\right)^{3.2} \{1 - \sqrt{1 - \alpha_1^2}\}^2 + k^{3.2} \{\text{arc sin } \alpha_1\}^2 \right] \times \sqrt{1 - k^2 \cos^2 \phi} \quad (52)$$

As indicated previously, the method does not anticipate use of Equation (52) except for values of ϕ in the range from 60° to 120° . Equation (52) approaches correct values in the limits of $k = 0$ and $k = 1$. As α_1 approaches unity, the K values given by Equation (52) are correct to about one percent. Comparisons to determine the accuracy of the equation for α_1 values less than unity are not available at the present time. However, from general considerations, the accuracy of the equation should be adequate for practical situations such that the crack-absent stress pattern seems appropriate for use of this approximation method. Methods of extending use of Equation (52) to situations where the crack-absent value σ_2 changes continuously as a function of α are well known and need not be detailed here.

B. Method B

As indicated in Section 2.A, an exact weight function method is available for an arbitrary "no-crack" normal stress field, σ_2 , in the special case where the flat-elliptical crack is circular. For the circular crack, the complete elastic solution is available for the

problem where a pair of splitting forces of magnitude P are applied at a point B on the crack surfaces as shown in Figure 10 or Figure 27⁹.

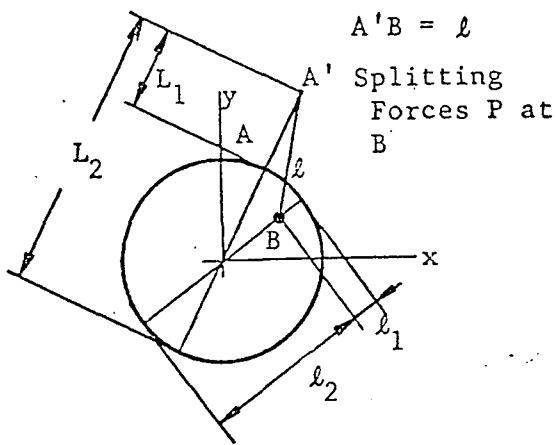


Figure 27

The normal stress σ_z at A' on the plane of the crack is written as follows:

$$\sigma_{z \text{ at } A'} = \frac{P}{\pi} \frac{1}{l^2} \frac{\sqrt{l_1 l_2}}{\sqrt{L_1 L_2}} \quad (53)$$

where the lengths l , l_1 , l_2 , L_1 , and L_2 are shown in Figure 27.

The stress intensity factor at A given by Equation (21) was obtained from Equation (53).

As a method for obtaining a plausible estimate of K for an elliptical crack, the following procedure can be used. Assume the expression for σ_z , given by Equation (53), remains nearly valid if Figure 27 is expanded uniformly in the x direction so that the perimeter of the crack has the shape of an ellipse. The length factors in Equation (53)

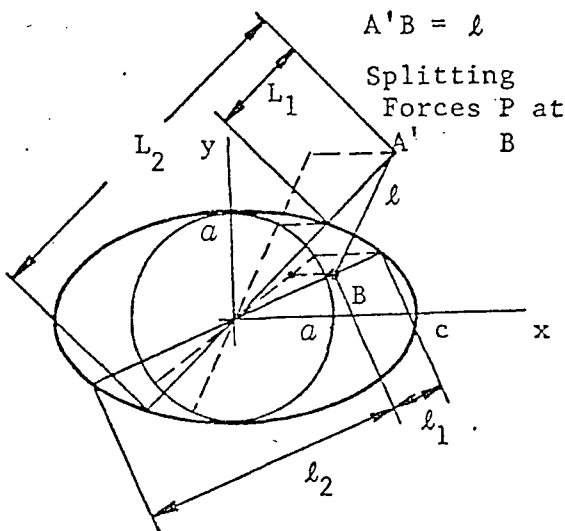


Figure 28

are straight line segments shown in Figure 28 after such a modification of the figure. Assume next that the K value at the new location A for splitting forces P at the new location B can be derived in the usual manner using Equation (53) and the definition equation:

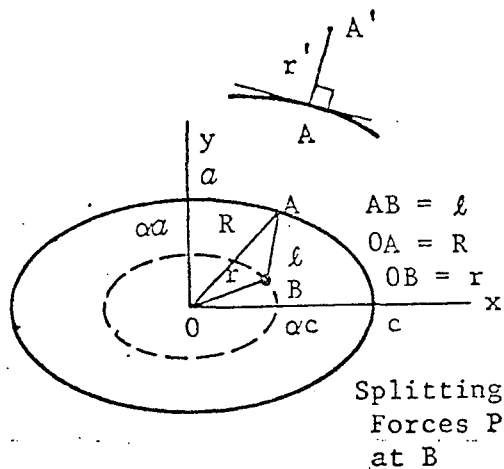


Figure 29

The details of this derivation can be omitted here. The resulting value for K at a boundary point A corresponding to a parametric angle ϕ was found to be given by

$$K = \frac{P \sqrt{a}}{\pi^{3/2} \ell} \sqrt{\frac{r}{R}} \frac{\sqrt{\frac{1}{\alpha^2} - 1}}{\{1 - k^2 \cos^2 \phi\}^{1/4}} \quad (55)$$

The lengths ℓ , r , and R are shown in Figure 29. The parameter α designates an ellipse, similar in shape to the perimeter of the crack, which passes through the point B . In other words, from Equation (49), the location, B , of the splitting forces is designated by values of α and ϕ_1 in the equations

$$x = \alpha c \cos \phi_1, \quad y = \alpha a \sin \phi_1 \quad (56)$$

The parameters k and ϕ have the same meaning as in Method A (see Figure 24, Equations (46) and (47)).

The accuracy of Equation (55) is exact for $a = c$ and $k = 0$, and the loss of accuracy for moderate increases of k would be expected to be relatively small. Numerical integration trials were made for

$$K = \text{Limit}_{r' \rightarrow 0} \sigma_z \sqrt{2 \pi r'} \quad (54)$$

where the limit process represents movement of point A' toward coincidence with point A , r' is the distance between A and A' , and AA' is normal to the ellipse at point A as shown in Figure 29.

the constant no-crack normal stress, $\sigma_z = \sigma$, so that exact answers would be available for comparison. When $c = 2a$ was assumed, the K values resulting from Equation (55) turned out to be, on average, about 7 percent high for $\bar{\phi} = 0^\circ$, 60° , and 90° . Additional numerical estimates were made using a linear decrease of the no-crack two-dimensional normal stress σ_z in the form

$$\sigma_z = \sigma \left(1 - \frac{|y|}{a}\right) \quad (57)$$

The only available comparison estimates for this stress distribution are in the form of rough estimates by Merkle^{2,3} which assume the line $y = 0$ is a free boundary and include a free surface correction. Allowing for the free surface correction, the comparison at $\bar{\phi} = 90^\circ$ showed approximate agreement. The comparisons at $\bar{\phi} = 60^\circ$ and at $\bar{\phi} = 0^\circ$ suggested that the results from Equation (55) were increasingly high (by comparison with Merkle) as the parametric angle $\bar{\phi}$ decreased from 90° .

Considering the nature of the calculations which can be made using Methods A and B, these two methods appear suitable for making lower bound and upper bound estimates of K for a rather extreme type of stress non-uniformity as represented by Equation (57). In practical applications, a smaller degree of stress non-uniformity is expected and the angle $\bar{\phi}$ of main interest will usually be close to the value $\bar{\phi} = 90^\circ$.

C. Free Surface Correction Factors

The K values from Methods A and B require application of free surface correction factors. With regard to free surfaces intersected by the leading edge of the crack, the K value derived by the methods discussed above essentially assume zero normal displacements on the free surfaces. In other words, the free surfaces are assumed to be planes of symmetry ($\tau_{yz} = 0$) relative to the stress pattern of the completely embedded crack. To allow for zero normal stress rather than zero normal displacements on the free surfaces, the K value derived assuming zero normal displacements should be multiplied by a factor moderately larger than unity. From such calculations as are available, the range of this free surface correction is from 1.0 to 1.3. This correction factor can be estimated uniformly as 1.15 with assurance that the estimate will rarely be in error by more than 5 percent. The correction factor tends to increase with the degree of concentration of the no-crack stress σ_z close to the free surface. However, situations of this kind sufficiently extreme to justify use of a correction factor larger than 1.2 are rare and should not be present for cracks of interest in welded steel bridge components. From these considerations, it is believed that the task of selecting an appropriate free surface correction factor can be settled in a simple and convenient manner by consistent use of the 15 percent elevation provided by the correction factor, 1.15, as noted above.

When a surface crack in a plate becomes deep and the net ligament becomes less than the crack depth, consideration can be given to a second kind of free surface correction factor. This factor is

sometimes referred to as the correction factor for the "back" free surface. An approximate estimate of the back free surface correction factor, F_B , can be made by the equation

$$F_B = \sqrt{\frac{2B}{\pi a} \tan \frac{\pi a}{2B}} \quad (58)$$

where a is the crack depth and B is the plate thickness. However, the correction factor F_B given by Equation (58) should be used with caution. When the k value for the elliptical shape of the crack is not far from unity, Equation (58) will provide an overestimate of F_B . In addition, attention must be given to situations such that the net ligament is small enough so that general yielding occurs. In such cases a different approach using a plasticity type characterization of the crack tip region should be used.

In the case of surface cracks at one end of a coverplate, at a web-flange junction, or at one end of a lateral attachment to a flange, the free surface intersected by the leading edge of the crack are usually restrained by the stiffness of a member attached to the flange by fillet welding. In such cases exercise of judgment in application of free surface correction factors is desirable. It is possible that, after consideration of the balance between displacement restraints and free surface effects, the best estimate of F_B might be unity.

Assuming that a reasonable number of abrupt fractures occur during this project from part-through surface cracks, the work of this project provides a valuable learning period on methods of K value estimation. During this learning period, use of upper and lower bound estimates along with additional study of estimation methods will be

of special value. Although a capability for making appropriate estimates of K for the various expected surface crack is available, additional study is needed to develop and select estimation methods which possess optimum combinations of accuracy and convenience.

4. SUMMARY

In this report, analytical studies were made for cracks with various geometric and loading configurations which may be encountered in bridge structures. The crack geometries treated in this report include two-dimensional edge cracks in half-plane and in a long strip, three-dimensional half-circular and quarter circular surface cracks, and quarter-circular and quarter-elliptical corner cracks.

To assist an understanding of the fracture failures in terms of failure load and fracture toughness, methods for estimating K values for these cracks with sufficient accuracy were discussed. For convenience of practical applications, approximate formulas for K were presented for many cases. Simplification of K-estimation methods was also discussed.

References which seem to be helpful for the surface crack analysis were listed at the end of the report following the direct references used in the present study.

5. REFERENCES

A. References Directly Used in the Report

1. Irwin, G. R.
"Crack Extension Force for a Part-through Crack in a Plate",
Journal of Applied Mechanics, Vol. 29, Trans. ASME, Vol.
84, Series E, 1962, pp. 651-654
2. Merkle, J. G.
"A Review of Some of the Existing Stress Intensity Factor
Solutions for Part-through Surface Cracks",
ORNL-TM-3983, Oak Ridge National Laboratory, Oak Ridge,
Tennessee, January 1973
3. Merkle, J. G.
"Stress Intensity Factor Estimates for Part-through Surface
Cracks in Plates, Under Combined Tension and Bending",
Oak Ridge National Laboratory, Oak Ridge, Tennessee,
September 1974
4. Tada, H., Paris, P. and Irwin, G.
"The Stress Analysis of Cracks Handbook",
Del Research Corporation, Hellertown, Pa., 1973
5. Emery, A. F., Walker, G. E., Jr. and Williams, J. A.
"A Green's Function for the Stress-Intensity Factors of
Edge Cracks and Its Application to Thermal Stresses",
Trans. ASME, Series D, Journal of Basic Engineering,
Vol. 91, pp. 618-624
6. Smith, F. W., Emery, A. F. and Kobayashi, A. S.
"Stress Intensity Factors for Semi-Circular Cracks-Part 2-
Semi-Infinite Solids",
Journal of Applied Mechanics, Vol. 34, Trans. ASME,
Series E, Vol. 89, 1967, pp. 953-959
7. Tracy, D. M.
"3-D Elastic Singular Element for Evaluation of K Along
an Arbitrary Crack Front"
International Journal of Fracture, Vol. 9, 1973, pp.
340-343
8. Kobayashi, A. S. and Enetanya, A. N.
"Stress Intensity Factor of a Corner Crack"
Presented at 8th National Symposium on Fracture Mechanics,
Brown University, August 1974

9. Galin, L. A.
"Contact Problems in the Theory of Elasticity"
GITTL, M., 1953 (in Russian)
Translation: North Carolina State College Publications,
1961

B. Other References which seem to be helpful to the surface crack analysis are listed below.

10. Kobayashi, A. S. and Moss, W. L.
"Stress Intensity Magnification Factors for Surface-Flawed Tension Plate and Notched Round Tension Bar",
Proceedings of the Second International Conference on Fracture, Brighton, England, 1969
11. Shah, R. C. and Kobayashi, A. S.
"Stress Intensity Factor for an Elliptical Crack under Arbitrary Normal Loading",
Journal of Engineering Fracture Mechanics, Vol. 3, 1971, pp. 71-96
12. Shah, R. C. and Kobayashi, A. S.
"On The Surface Flaw Problems"
The Surface Crack: Physical Problems and Computational Solutions, edited by J. L. Swedlow, ASME, 1972, pp.79-124
13. Smith, F. W. and Alair, M. J.
"Stress Intensity Factors for a Part-Circular Surface Flaw",
Proceedings of the First International Conference on Pressure Vessel Technology, Delft, Holland, 1969
14. Smith, F. W.
"The Elastic Analysis of the Part-Circular Surface Flaw Problems by the Alternating Method",
The Surface Crack: Physical Problems and Computational Solutions, edited by J. L. Swedlow, ASME, 1972, pp. 125-152
15. Thresher, R. W. and Smith, F. W.
"Stress Intensity Factors for a Surface Crack in a Finite Solid"
Journal of Applied Mechanics, Vol. 39, Trans. ASME, Series E, 1972, pp. 195-200.
16. Hartranft, R. J. and Sih, G. C.
"Alternating Method Applied to Edge and Surface Crack Problems"
Mechanics of Fracture I - Methods of Analysis and Solutions of Crack Problems, edited by G. C. Sih, Noordhoff International, 1973, pp. 179-238

17. Nishitani, H. and Murakami, Y.
"Stress Intensity Factors of an Elliptical Crack or a Semi-Elliptical Crack Subject to Tension",
International Journal of Fracture, Vol. 10, 1974,
pp. 353-368
18. Rice, J. R. and Levy, N.
"The Part-through Surface Crack in an Elastic Plate",
Journal of Applied Mechanics, Vol. 39, Trans. ASME,
Series E, 1972, pp. 185-194
19. Rice, J. R.
"The Line Spring Model for Surface Flaws"
The Surface Crack: Physical Problems and Computational;
Solutions, edited by J. L. Swedlow, ASME, 1972
20. Miyamoto, H. and Miyoshi, T.
"Analysis of Stress Intensity Factor for Surface-Flawed
Tension Plate"
High Speed Computing of Elastic Structure, Proc. of
Symposium of IUTAM, University de Liege, 1971, pp.
137-155
21. Smith, F. W.
"Stress Intensity Factors for a Surface Flawed Fracture
Specimen",
Technical Report No. 1, Department of Mechanical
Engineering, Colorado State University, September 1971
22. Newman, J. C.
"Fracture Analysis of Surface-and Through-Cracked Sheets
and Plates",
Engineering Fracture Mechanics, Vol. 5, 1973, pp. 667-690
23. Marrs, G. R. and Smith, C. W.
"A Study of Local Stresses Near Surface Flaws in Bending
Fields"
Stress Analysis and Growth of Cracks, ASTM STP513, 1972,
pp. 22-36
24. Schroedl, M. A. and Smith, C. W.
"Local Stresses Near Deep Surface Flaws Under Cylindrical
Bending Fields",
Progress in Flaw Growth and Fracture Toughness Testing,
ASTM STP536, 1973, pp. 45-63
25. Harms, A. E. and Smith, C. W.
"Stress Intensity Factors for Long, Deep Surface Flaws
in Plates Under Extensional Fields",
VPI-E-73-6, Virginia Polytechnic Institute and State
University, Blacksburg, Virginia, February 1973